Department of Human and Engineered Environmental Studies
Graduate School of Frontier Sciences
The University of Tokyo

2022

Master's Thesis

Dependence of Rhythmic Precision on Synchronization in Oscillator Networks

（振動子ネットワークにおけるリズム精度の同期依存性）

Submitted on September 2, 2022
Adviser: Professor Hiroshi Kori

平田 幸子
Sachiko Hirata

Abstract

Varieties of rhythmic dynamics are observed in nature. Particularly, biological rhythms, such as circadian rhythms, neuronal firing, or heartbeats are thought be important for the maintenance of vital activities and the rhythmic precision (temporal precision) of the periodicity should be assured stably.

Here in this thesis dependence of temporal precision on synchronization level in oscillator network was investigated on various network parameters, including network size, coupling strength, the Kuramoto order parameter, and the network topology.

The coefficient of variation (CV) for cycle-to-cycle periods of collective oscillation directly indicates the temporal precision, whereas the reciprocal index $1/\tau$ of exponential decay of autocorrelation also teaches the same scientific knowledge.

CV-R curve directly shows the dependence of temporal precision on synchronization and the result shows that collective enhancement of the temporal precision is suggested, and beside these other certain uncovered relations might exist between CV and R, i.e., temporal precision and the synchronization.

Keywords: Kuramoto model, synchronization, temporal precision, collective enhancement, network topology

Index

Section 1. Introduction

Varieties of rhythmic dynamics are observed in nature. Biological rhythms, such as the firefly luminescence, circadian rhythms, neuronal firing, or heartbeats, as well as non-biological rhythms, such as oscillation of pendulum clock or mechanical metronome have the periodical dynamics [1-5].

Synchronization is a phenomenon, in which a group of self-sustained oscillators begin to have the same oscillation timing by some interaction or periodic external force [6,7]. Biological rhythms are created by synchronization of biological oscillators. Precise periodicity in biological rhythms, so called rhythmic precision or temporal precision of collective oscillations is thought to be important for the maintenance of vital activities.

Synchronization and temporal precision are distinct properties. Synchronization is indicated by the amplitude of the collective oscillation (FIG.2), whereas the temporal precision is indicated by the periodical accuracy of collective oscillation. Even when ensemble of oscillators synchronizes, it is not certain whether temporal precision is also assured [8-10].

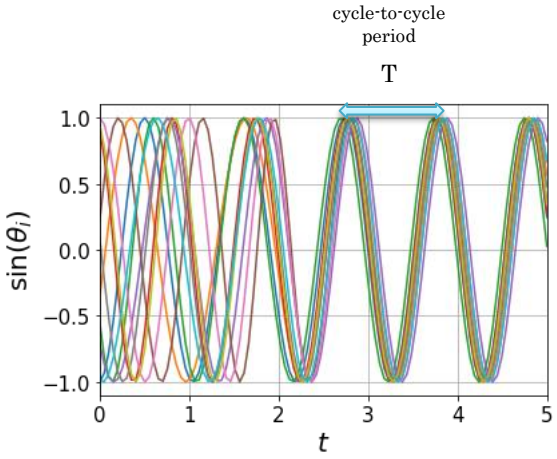

FIG1. Synchronization and temporal precision in oscillator network

Synchronization level is represented symbolically as a bundle of oscillating sign curves, whereas the rhythmic accuracy (rhythmic precision, clock precision or temporal precision in other words) is interpreted as the accuracy of cycle-to-cycle periods of the collective oscillation. As shown, synchronization and temporal precision are distinct properties. The number of oscillators is 10 (N=10).

Rhythmic accuracy can be easily measured by experimentation. Historically, many experiments had been attempted to explore the temporal precision of periodical phenomena, and

various experimental studies have been reported [11].

Particularly, collective enhancement of temporal precision, first reported in Biophysics J., 1979 is highly suggestive [12]. A study of rhythmic accuracy of cardiomyocytes is reported in this paper and the hypothesis says that the coefficient variation (CV) of periodical biological rhythm is proportional to the inverse of square root of the number of oscillators (N), i.e., CV$\propto 1/\sqrt{N}$, which is reminiscent of the central limit theorem, though it is not trivial at all [13,14].

Arthur Taylor Winfree, who is the pioneer of phase description model for periodical dynamical system (Winfree model) expressed his opinion about the collective enhancement of temporal precision in his monograph (*The Geometry of biological clock*, 2nd, Springer, 2001) [2]: "But as far as I am aware, neither the physiological nor the mathematical essence of such a collective refinement mechanism has yet been revealed."

Winfree presented one theoretical building for dealing with coupled systems of limit-cycle oscillators. This method describes oscillational phenomena with only one degree of freedom, i.e., degree of phase [1,2].

Yoshiki Kuramoto modified the Winfree model to create Kuramoto model. Kuramoto introduced so-called "the phase reduction method" to simplify the Winfree's nonlinear equation. Kuramoto showed for the first time theoretically that synchronization of oscillators occurs in second order phase transition in the thermodynamic limit of $N \to \infty$, that is now world-wide known as "Kuramoto transition" [3,7,15-18]. Nonetheless, in the real world, rhythmic phenomena, especially biological rhythms, or nonlinear dynamical motions are taken on finite number of oscillators, next the finite size effect as well as the finite size scale transformation have been studied [19-24].

In the course of the history thus far many studies had been done for Synchronization transitions of Kuramoto oscillators on networks. On the other hand, not many studies had been attempted on the fluctuations of the rhythm in Kuramoto model. There are few previous studies on rhythmic accuracy in mathematical models. Fluctuations are very important in terms of system functioning. Synchronized network with high synchronization level is not always functional if fluctuations are large.

The relationship between rhythmic accuracy and the synchronization is reported precisely in Kori. et. al. 2012.[10] (Hereinafter referred as Ref. [10]). Dependence of temporal precision on oscillator population size N was verified in mathematical physics, using the self-sustained coupled oscillator model, i.e., Fitzhugh-Nagumo equation, the circadian rhythm model, and the Stuart Landau Oscillators, and numerical analysis as well as the theoretic formulae were derived. Assuming the phase identical situation with weak noise added, the regularity of oscillatory dynamics clearly showed the collective enhancement of temporal precision certainly in the numerical and theoretical analyses. Dependence of temporal precision on network topology is also indicated as such; when the network structure is suitable for synchronization (e.g., all-to-all network), the rhythmic accuracy of collective oscillation on the network is very precise, whereas the network structure is not suitable for synchronization (e.g., ring-connection, scale-free network, small world network etc.), rhythmic accuracy decreases.

The preceding study Ref. [10] is one of the first attempts of mathematical and theoretical studies of temporal precision of oscillator networks, and my study is aiming for the same goal but from different perspectives.

In Ref. [10] assuming weak random noise and identical oscillators with identical frequency, the mathematical model was linearized to be treated as multivariate Ornstein-Uhlenbeck process to achieve the theoretical findings. However, when the random noise is not weak, the linearization is no longer a good approximation. Besides the oscillators in nature are not identical, but have dispersed natural frequencies, often the dispersion function is unimodal function such as Gaussian distribution.

In my study, as a continuation of studies in Ref. [10], I investigated the oscillation regulatory of non-linear process of synchronization of dispersed coupled phase oscillators. Theory of Kuramoto model handles the phase equations for oscillators with dispersed natural frequencies, and the oscillation regulatory of the non-linear process of synchronization, above all near the onset of the synchronization is the subject of this study. Specifically, dependence of rhythmic precision on synchronization of self-sustained coupled phase oscillators was investigated on various network parameters, including network size, coupling strength, and the network topology.

Section2. Background Art

2.1 Winfree model

An attempt to describe oscillators in terms of phase is first made by A. T. Winfree [1].

In general, oscillatory motions have two degrees of freedom: phase and amplitude, and if the oscillator receives action from the oscillators or outside the system, both phase and amplitude will change. However, nonlinear oscillations have a characteristic form of oscillation called limit-cycle oscillation, in which the state of the system converges to a certain attractor trajectory (limit-cycle) in phase space, and the limit-cycle motion has orbital stability.

A self-sustained oscillator is described as a limit-cycle attractor. Assume that when the oscillator is isolated, the velocity of phase ϕ $(0 \leqq \phi < 2\pi)$ is constant, denoted by natural frequency ω, i.e.

$$\frac{d\phi}{dt} = \omega_{const.}. \tag{1}$$

When stimulus or perturbation is given to the oscillator, the time evolution of phase may increase or decrease depending on the instantaneous phase,

$$\frac{d\phi}{dt} = \omega + \kappa z(\phi)p(t), \tag{2}$$

where $p(t)$ is a function depending on time, $z(\phi)$ is a phase response curve or phase sensitivity function, and κ is a parameter that indicates the strength of perturbation.

This phase equation is called Winfree type phase model [1,2,3,17,18].

2.2 Kuramoto model

When $p(t)$ is a periodical function, $p(t)$ can be described as $p(t) = q(\phi')$, $\phi' = \Omega t$, and the second term of the Winfree type phase equation can be time-averaged for a limit-cycle period T to be converted to a simpler expression $f(\phi - \phi')$;

$$Z(\phi - \phi')\, q(\phi') \approx \frac{1}{T}\int_0^T Z(\phi + \omega t)\, q(\phi' + \omega t)\, dt = f(\phi - \phi'). \tag{3}$$

Kuramoto Sakaguchi model or Kuramoto model (when $\alpha = 0$) is such converted and simplified type of Winfree type model where $f(\phi - \phi')$ is chosen to $sin(\phi - \phi')$:

$$\frac{d\phi_i}{dt} = \omega_i + \frac{K}{N}\sum_{j=1}^{N} A_{ij} \sin\left(\phi_j - \phi_i - \alpha\right), \tag{4}$$

where ϕ_i is phase, ω_i is the natural frequency, K is a coupling strength, N is network size (number of oscillators in an ensemble), and $\sin(\phi_j - \phi_i)$ is the periodical perturbation term from the original Winfree model [3,7,15-18]. Hereinafter, both Kuramoto-Sakaguchi model and Kuramoto model are referred to as Kuramoto model.

Kuramoto model handles oscillators with dispersed natural frequencies. The dispersion function is assumed to be a unimodal function, and its momentum feature affects considerable influences on other parameters of the phase equation. A shift in the expectation (first momentum feature) corresponds to a shift of ω_i itself, and a shift in the variance (second momentum feature) corresponds to a shift in the value of the coupling strength K. A shift in the skewness (third momentum feature) corresponds to a shift in the minimum amplitude of the collective oscillation $R_{\min}$, and a shift in kurtosis (forth momentum feature) corresponds to a shift in the frequency $\langle\dot{\psi}\rangle$ of the collective oscillation [24].

A_{ij} is an adjacent matrix which reflects the network topology to the interaction of oscillators. If there is a link between oscillator i and oscillator j, 1 is set as a matrix element A_{ij}, and if there is no link, 0 is set. An undirected graph yields a symmetric matrix, and a directed graph yields an asymmetric matrix. If the interaction is a negative action, then -1 can be set for the interaction. In this study, since anything other than undirected and positive interactions are not considered, the adjacent matrix A_{ij} is assumed to be non-negative symmetric matrix.

2.3 Synchronization

Synchronization is a physical phenomenon, in which a group of self-sustained oscillators begins to have the same oscillate timing by some interaction or periodic external force.

Consider a network of coupled phase oscillators: the collective state at a given time of a network with N limit-cycle oscillators can be represented by a dispersion of N points on the complex unit circle. The complex order parameter Z is defined as mean or centroid of complex coordinates of the oscillators, and the Kuramoto order parameter R is the amplitude of the complex order parameter.

$$Z = Re^{i\psi} = \frac{1}{N}\sum_{j=1}^{N} e^{i\phi_j} \tag{5}$$

When the oscillators are in asynchronous state, oscillators are scattered over the complex unit circumference, and R is close to zero. When the oscillators are becoming synchronized, R becomes closer to 1. Hence, the Kuramoto order parameter R indicates the degree of synchronization of coupled phase oscillators. In this study, the Kuramoto order parameter R is used as an index of synchronization level.

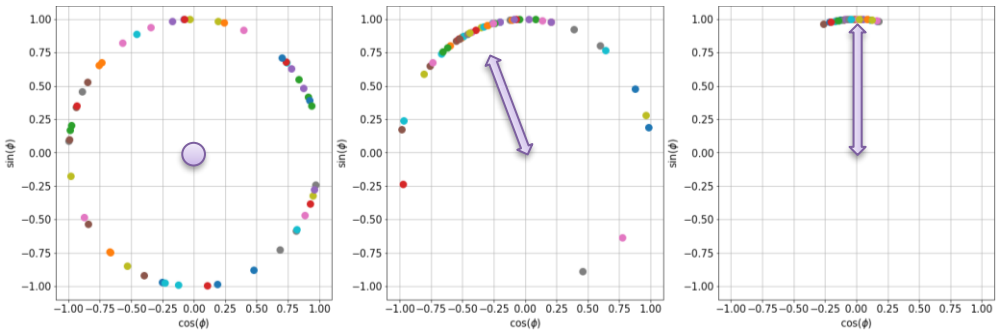

R≅0 R≅0.6.~0.7 R≅1

FIG. 2. Kuramoto order parameter *R*

N oscillators are dispersed over the complex unit circumferences, and the amplitude of the mean coordinate is shown in the violet arrows. *R*=0 corresponds to a disordered state, and *R*=1 corresponds to a state of perfect phase identical state.

Fig.3 shows the value of Kuramoto order parameter R for various coupling constant K and network size N in Kuramoto model. The $R-K$ curve is interpreted as the dependence of synchronization level on the coupling strength K, and R is interpreted as an index of synchronization level for given K value.

Interestingly, when $K=0$, the Kuramoto order parameter R is not zero, though interactions of oscillators do not exist. This is due to the dispersed natural frequencies and the finite size effect. As shown, a network with 100 oscillators (N=100) has $R \cong 0.1$, and it is generally said that network with N oscillators has the order parameter $R \cong 1/\sqrt{N}$ because of law of large numbers and central limit theorem [22-24].

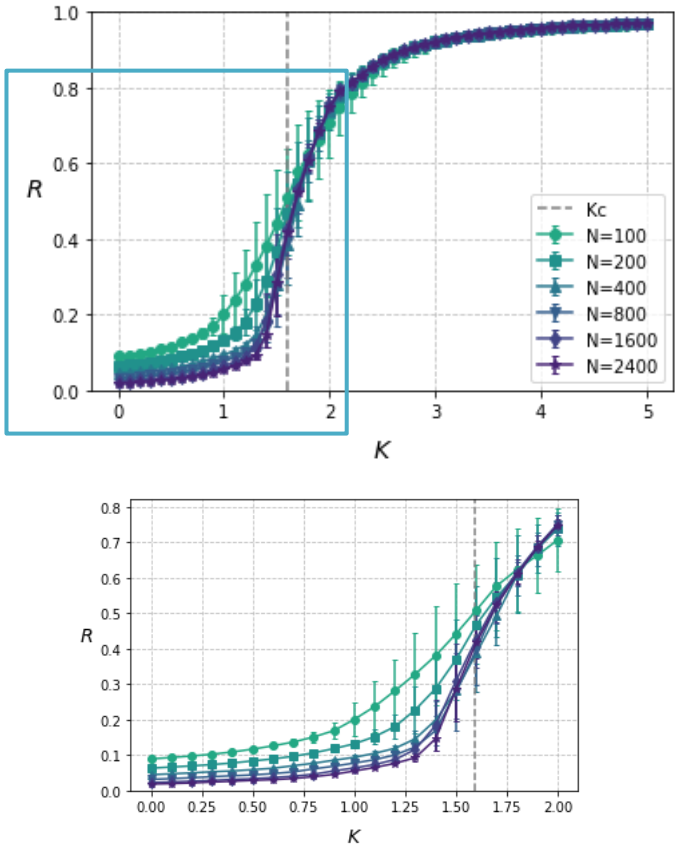

FIG. 3. Dependence of synchronization level *R* on the coupling strength *K* in Kuramoto model
Synchronization transition of finite size Kuramoto phase oscillators occurs near the critical coupling strength Kc. Kuramoto model with the natural frequency $g(\omega) \sim \mathcal{N}(2\pi, 1)$, All-to-all network, average of 10 trials. The lower figure is the enlarged view of the squared area (K=0~2).

Kuramoto model treats various quantities theoretically, assuming the thermodynamic limit $N\to\infty$ and $t\to\infty$. In the thermodynamical limit, the synchronization transition (Kuramoto Transition) may occur when the coupling strength K is stronger than the threshold value. i.e., the critical coupling strength K_c. The order parameter R is given by the polynomial of R itself in the form of self-consistent equation,

$$R = \int_{|\omega_i-\Omega|} d\omega g(\omega) \sqrt{1-\left(\frac{\omega}{KR}\right)^2}, \tag{7}$$

and the critical coupling strength K_c is given by

$$K_c = \frac{2}{\pi g(\bar{\omega}),} \tag{8}$$

where $g(\bar{\omega})$ is the peak value of the unimodal dispersion function $g(\omega)$ of the natural frequency. Without losing generality, a parallel shift of the coordinates of $\bar{\omega}$ to $\bar{\omega}=0$ may be performed,

$$K_c = \frac{2}{\pi g(0)} \tag{9}$$

when the dispersion function $g(\omega)$ is the gaussian function $\mathcal{N}(0,1)$, $g(0)=1/\sqrt{2\pi}$ and K_c is estimated to $K_c \approx 1.6$.

Though the critical coupling strength K_c is a threshold parameter assuming the thermodynamical limit, synchronization transition occurs similarly near $K \approx K_c$ in the finite size networks as shown in Fig.3. When K is slightly smaller than K_c, the Kuramoto order parameter R corresponds to $R = 0.2\sim0.4$, which is referred to “onset of the synchronization”.

An all-to-all network model in which one oscillator is congruent with all other oscillators with the same strength is also known as a mean-field model. In the mean-field model, behaviors of all the oscillators are dominated by a mean-field oscillation, which is yielded by the sum of all oscillators in the population. Considering the mean-field oscillation as an external force, phase equation for the individual oscillator is given by Kuramoto-Sakaguchi model:

$$\frac{d\phi_i}{dt} = \omega_i + KR\sin(\phi_j - \psi - \alpha), \tag{10}$$

where R is amplitude and ψ is phase of the mean-field oscillation.

2.4 Number of synchronized oscillators

By the virtue of theoretical aspects of Kuramoto model, number of synchronized oscillators on the all-to-all network can be calculated from the coupling strength K and the mean-field amplification R.

Phase oscillators on the all-to-all network interacting with the mean-field oscillation (with amplitude R and frequency Ω) according to the equation (10) are divided into two groups, synchronized group and non-synchronized group, according to the natural frequency ω_i;

when $KR > |\omega_i - \Omega|$, the oscillator belongs to the synchronized group; and

when $KR < |\omega_i - \Omega|$, the oscillator belongs to the non-synchronized group [7].

Along with this theory, the number of synchronized oscillators (*Ns*) with the natural frequency dispersion $\mathcal{N}(0,1)$ can be calculated as:

$$N_s = N \int_{-KR}^{KR} \frac{1}{\sqrt{2\pi}} \exp\left(-\frac{\omega^2}{2}\right) d\omega. \tag{11}$$

Fig.4 shows calculated KR values from R and K in Fig.3.

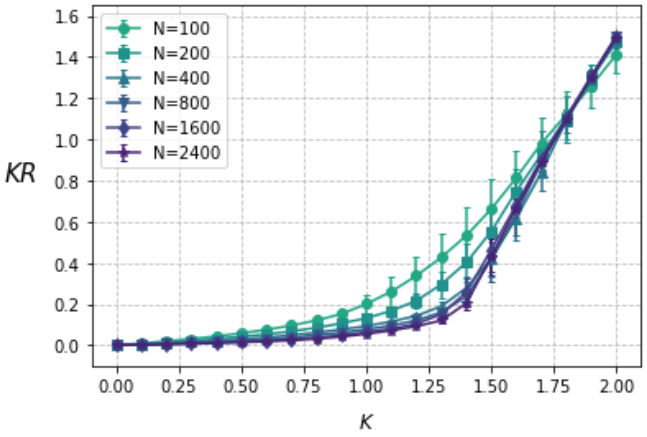

FIG. 4. Calculated KR values of mean-field oscillation for various network size N

When K is near 1.7-1.8, KR is near 1. According to the equation (11) and with the reference to 1σ of normal distribution $\mathcal{N}(0,1)$, the number of synchronized oscillators can

be estimated to about 68% (Ns/N≈0.68).

When K is near 2, KR becomes $KR \approx 1.5$. According to the equation (11) and with the reference to 1.5σ of normal distribution $\mathcal{N}(0,1)$, the number of synchronized oscillators can be estimated to about 86.6% (Ns/N≈0.866).

In this way numbers of synchronized oscillators are calculated, and the result is shown in Fig. 5. Though the Kuramoto theory assuming the thermodynamical limit $N \to \infty$ explains the occurrence of second order phase transition, in the finite size network synchronization occur thresholdlessly. and the ratio of synchronized oscillators is gradually increasing.

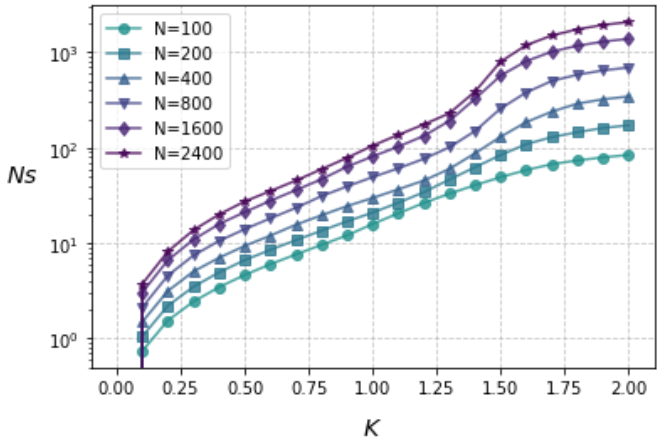

FIG.5 Numbers of synchronized oscillators

Numbers of synchronized oscillators are estimated according to the equation (11).

2.5 Noisy Kuramoto model

Noise causes phase-diffusion and induces irregularity in oscillation. Hence Kuramoto model considers the noise term [6,7].

A phase equation for noisy Kuramoto model is given by:

$$\frac{d\phi_i}{dt} = \omega_i + \frac{K}{N}\sum_{j=1}^{N} A_{ij}\sin(\phi_j - \phi_i) + \sqrt{D}\xi_i\,, \tag{12}$$

where ω_i, K, N, and A_{ij} are the same as the phase equation (4), D is a noise strength parameter and ξ_i is independent noise, e.g., white Gaussian noise.

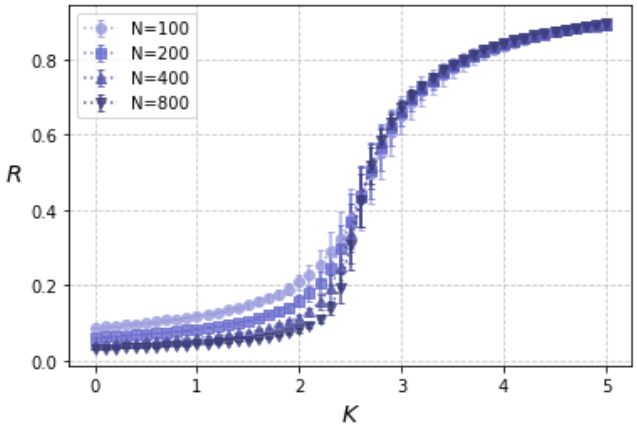

FIG. 6. Synchronization level in noisy Kuramoto model

Fig.6 shows the synchronization of noisy Kuramoto model with the natural frequency $g(\omega)\sim\mathcal{N}(2\pi, 1)$ and random gaussian noise $E[\xi_i(t)] = 0$, $E[\xi_i(t)\xi_j(t')] = \delta_{ij}\delta(t-t')$, with the noise strength parameter $\sqrt{D} = 1$. With such moderate (not weak) noise, synchronization is unlikely to occur when the coupling strength K is weak, henceforth sufficient strong coupling strength should be given to observe the phase transition. The critical coupling strength K_c is in this case $K_c \cong 2.5$ for the phase-disturbance caused by noise.

2.6 Noisy and frequency-identical oscillators

Certainly noisy Kuramoto model is the best mathematical model for analyzing synchronous phenomena in nature, historically frequency-identical cases were also well studied. The phase equation is same as shown for noisy Kuramoto model, the only difference is that the natural frequency ω is not dispersed, but identical for all oscillators (as defined):

$$\frac{d\phi_i}{dt} = \omega_{cosnt.} + \frac{K}{N}\sum_{j=1}^{N} A_{ij}\sin(\phi_j - \phi_i) + \sqrt{D}\xi_i\,. \tag{13}$$

This equation is comprehended as a non-linear Fokker Planck equation. If the noise term $\sqrt{D}\xi_i$ is weak, the equation can be linearized and comprehended as multivariate Ornstein-Uhlenbeck process [25]. Compared with the case of noisy Kuramoto model, synchronization occurs with weaker coupling strength K.

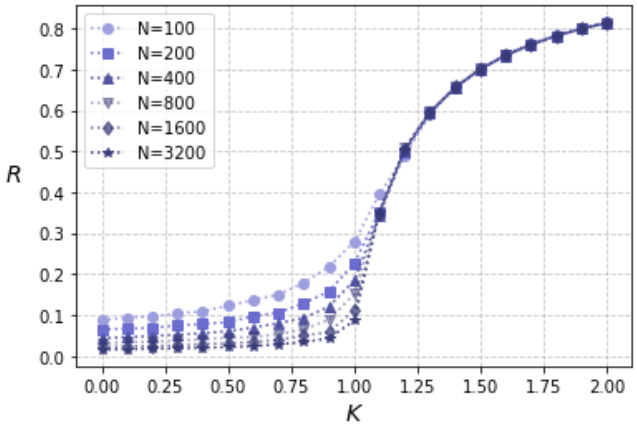

FIG7. Synchronization level in frequency identical phase oscillator

In this case the synchronization occurs $K \cong 1.0$ (The critical coupling strength $K_c \cong 1.0$).

2.7 Temporal precision

Coefficient of Variation (CV) of cycle-to-cycle periods is a direct parameter of temporal precision that can be compared with the experimentally measured values in various previous papers. CV is the standard deviation (SD) of the cycle-to-cycle periods divided by the mean period.

$$\mathrm{CV} = \frac{\mathrm{std[cycle\text{-}\ to\text{-}\ cycle\ periods]}}{\mathrm{mean[period]}} \tag{14}$$

Dependence on CV on the network size N is reported in Ref. [10];

(i) CV is proportional to $1/\sqrt{N}$ for small N values for each coupling strength K.

(ii) CV approaches a constant value for large N values for each K, i.e., there is a crossover.

(iii) the crossover points N^* increases with K.

One of the purposes of my study is to know whether the collective enhancement of the temporal precision can be observed in the Kuramoto phase transition, especially near the onset of the synchronization (K=1.2~1.6, or R=0.2~0.4, depending on the network). Hence CV is used as an index of temporal precision, while the crossover of CV or the crossover point N* reported in Ref. [10] is not considered in this study.

Also, the autocorrelation function is used to analyze the time series of periodic function. Periodicity can be easily verified by calculating the Autocorrelation of time series data of the mean-field phase ψ:

$$C(t') = \langle \psi(t)\psi(t-t') \rangle = \lim_{T\to\infty} \int_0^T \psi(t)\psi(t-t')\,\mathrm{d}t. \tag{15}$$

When the time series of $\psi(t)$ is plotted for the timesteps t, the autocorrelation function draws the periodic curve, and its envelope shows the exponential decay $C(t') = \exp(-t'/\tau)$ with the exponential index $-1/\tau$, where τ is referred to as the time constant. In this study, the reciprocal index $1/\tau$ is set to another index of temporal precision which indicates the rhythmic accuracy of collective oscillation.

2.8 Network topology

All-to-all network is the simplest representative among various complex networks in the world. There are many different complex networks in the world, e.g., random network, scale-free network, small-world network, square-lattice network, and ring connection network etc.

It is known that synchronization of oscillatory networks is highly dependent on the network structure [26-31]. Historically it has been known that synchronization is unlikely to occur in oscillatory networks with large internode distance $\langle d \rangle$ such as square lattices [32], and conversely networks with small internode distance $\langle d \rangle$ are likely to synchronize [33].

Various network parameters, such as network size *N*, average degree $\langle k \rangle$, average number of links $\langle L \rangle$, and average distance $\langle d \rangle$ influence the synchronization of collective oscillation [34].

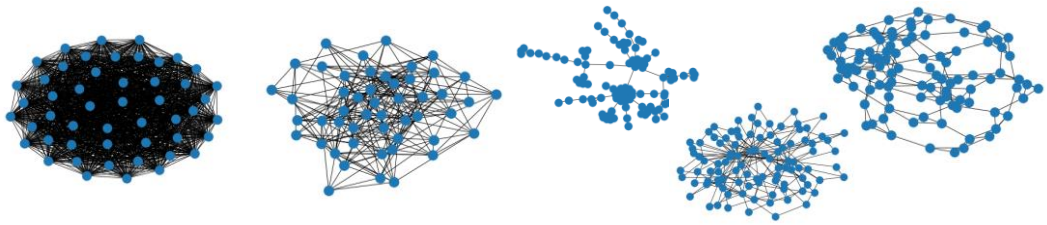

FIG. 8: Various oscillator network

All-to-all network, random network, scale-free network (m=1 or 2), small-world network.

Relationship between the average degree $\langle k \rangle$ of the network and the critical coupling strength K_c of the Synchronization transition is given from the mean field approximation [34]

$$K_c = \frac{2\langle k \rangle}{\pi g(0)\langle k^2 \rangle,} \tag{16}$$

where the dispersion of the degree is not considered.

All-to-all network has the average degree $\langle k \rangle = N - 1$, average number of links $\langle L \rangle = N(N-1)/2$ and the average distance $\langle d \rangle = 1$.

Random network has links for each combination of nodes (oscillators) at a rate of p ($0 < p < 1$). Random network has the average degree $\langle k \rangle = p(N-1)$, the average number of links $\langle L \rangle = pN(N-1)/2$, and the average distance $\langle d \rangle = \propto \ln N / \ln\langle k \rangle$. The phase equation of Kuramoto model is modified to quote the network parameter p,

$$\frac{d\phi_i}{dt} = \omega_i + \frac{K}{Np}\sum_{j=1}^{N} A_{ij}\sin(\phi_j - \phi_i). \tag{17}$$

Synchronization on random network is reported in Rodrigues et al., *Physics Reports* **610** (2016) 1–98[29] (Hereinafter referred as Ref. [29]). Fig. 9 is a result of numerical calculations according to the equation (17). As shown in the figure, dependence of synchronization level R on the coupling strength K is not affected by the network parameter p.

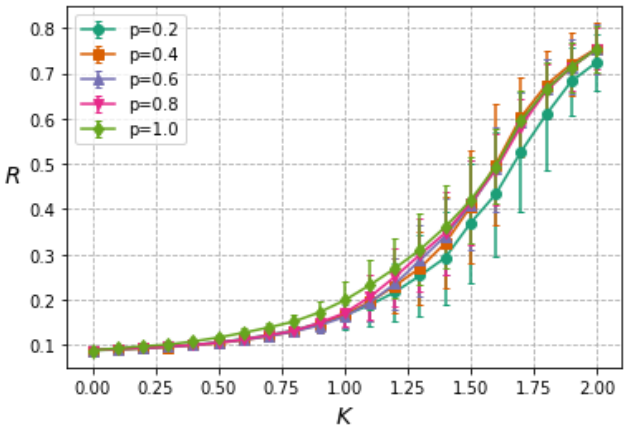

FIG. 9: Synchronization on Random network [29]

The Kuramoto order parameter R is plotted for the coupling strength K. Random network with different network parameter p has different sparseness. Random network with p=0.2 is the most sparce network, and random network with p=1.0 is equal to all-to-all network.

The next topic is Scale-free network, or so-called Barabási-Albert network named after the creator, A. Barabási L and R. Albert is another example of sparce network. Scale-free network has two distinct features, i.e., the network growth and preferential selection. Scale-free network is a growing network in which the nodes (vertices) of the network increase over time. And the preferential selection is a feature in which nodes with larger vertex orders are more likely to be connected at the edges [36,37], thus the graph node order becomes power distributed.

Scale-free network is observed everywhere in the world, i.e., electric power grid, paper citation relationships, web link relations, etc. The phase equation is given below, where ⟨k⟩ represents the average degree for each node in the network. ⟨k⟩=2 in scale free network.

$$\frac{d\phi_i}{dt} = \omega_i + \frac{K}{\langle k \rangle}\sum_{j=1}^{N} A_{ij}\sin(\phi_j - \phi_i), \tag{18}$$

Synchronization on scale-free network is reported also in Ref. [29]. Fig.10 is a result of numerical calculations according to the equation (18). As shown in the figure, oscillators on scale-free network hardly synchronizes even with very strong coupling strength K.

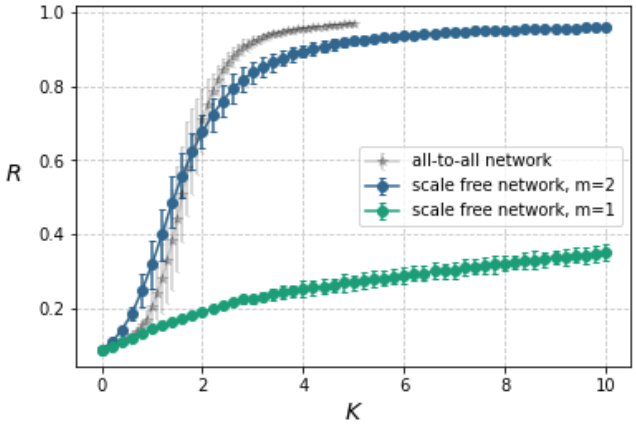

FIG. 10. Synchronization on Scale-free network [29]

Synchronization level is in scale-free network with m=1.0 is plotted for the coupling strength K. The mean values of 10 trials are shown with the standard deviations.

And the last topic is the Small world network. Small world network is first proposed by Watts and S. H. Strogatsz, as an extension of random network [38], characterized by coexistence of high clusterability and small mean distance. A small world network is made from 1-dimendional ring lattice connection and re-wiring the links with probability p. The phase equation is given by equation (18), where $\langle k \rangle$ is average degree and often $\langle k \rangle$=4. The re-wiring parameter p is related to the clusterability, when p increases, the clusterability decreases. Different from the scale free network, graph order is not power distributed in the small world network.

Synchronization on small world network is reported as well in Ref. [29]. Fig.11 is a result of numerical calculations according to the equation (18). As shown in the figure, oscillatory networks on small world network synchronizes, however with stronger K values.

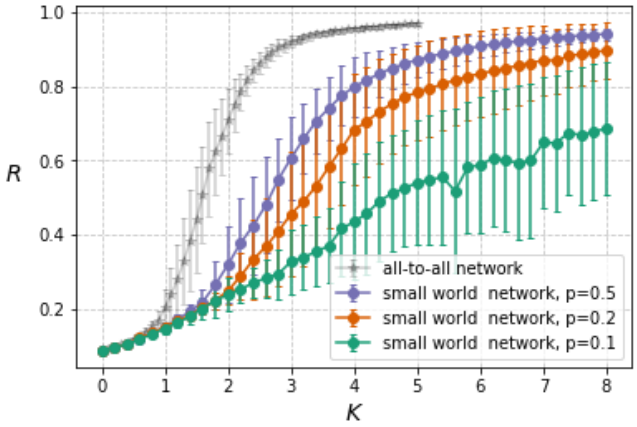

FIG. 11. Synchronization on Small-world network [29]

Synchronization level is in small world network with different order parameter is plotted for the coupling strength K. N=100, $\langle k \rangle$=4. The mean values of 10 trials are shown with the standard deviations.

Section.3 Subject of this study

The subject of my study is an inquiry of rhythmic precision of the collective mean-field oscillation in oscillatory networks. Dependence of temporal precision on synchronization level near the onset of the synchronization is inquired for the first time in this study.

In Ref. [10], assuming weak random noise and strong coupling strength K, the mathematical model was linearized to be treated as multivariate Ornstein-Uhlenbeck process. This assumption is corresponding to the coupling constant $K \to \infty$ and R=1. The onset of synchronization is highly non-linear and remained unstudied.

Mathematical models used in this study are below:

i. Kuramoto model (noiseless)
ii. noisy Kuramoto model; and
iii. noisy and frequency-identical phase oscillators.

Phase oscillators are assumed to be limit-cycle oscillators. The natural frequencies are assumed to be dispersed according to the unimodal gaussian function $g(\omega) \sim \mathcal{N}(2\pi, 1)$ in Kuramoto model (i and ii). The natural frequency is set identical in iii. The random gaussian noise $E[\xi_i(t)] = 0,\ E\left[\xi_i(t)\xi_j(t')\right] = \delta_{ij}\delta(t-t')$ with the noise strength parameter $\sqrt{D} = 1$ was added in noisy cases (ii. and iii.). The effect of noise will be known by comparing i. and ii., and the effect of dispersion on natural frequencies will be known by comparing ii. and iii.

CV is an orthodox parameter of temporal precision, whereas the autocorrelation of time series of mean-field phase is also a good indicator of temporal precision, especially, when oscillators have noise (ii and iii), since CV is hardly calculable for noisy phase oscillators. As described in the section 2, the autocorrelation shows the exponential decay with the index -1/τ. Hence 1/τ was set to another parameter which indicates the temporal precision.

Section.4 Results

4.1 Kuramoto model

Dependence of temporal precision of collective mean-field oscillation in Kuramoto model was investigated on all-to-all network. The results are shown in Fig. 12.

Dependence of CV (left column) and $1/\tau$ (right column) on the coupling strength K is shown in upper two figures (Fig.12a and Fig.12b). It is shown that CV-K curves and $1/\tau$-K curves have reverse-sigmoidal trajectories, CV and $1/\tau$ decrease as the coupling strength K increases. When the coupling strength K is larger than K_c (K_c<K), a network with larger network size system size N gives lower CV or $1/\tau$ values (better temporal precision), suggesting the existence of collective enhancement. On the contrary, when K is considerably smaller than K_c(K<K_c), a network with smaller network size N gives lower CV or $1/\tau$ values (better temporal precision). Remember that K_c is a threshold value under the thermodynamical limit (see eq. (9)), the behavior of CV-K curves and $1/\tau$-K curves have a considerable relevance to K_c. Specifically, there is a remarkable reciprocal intersect of CV-K curves and $1/\tau$-K curves in the vicinity of $K \cong K_c$, and this is discussed later in the section of Discussion.

Dependence of CV (left column) and $1/\tau$ (right column) on the synchronization level R is shown in middle two figures (Fig.12c and Fig.12d). It is shown that CV and $1/\tau$ decreases as the synchronization level (Kuramoto order parameter) R increases, suggesting that synchronization improves the temporal precision. A network with larger network size N gives lower CV or $1/\tau$ values (better temporal precision), for example network with 1600 oscillators has better temporal precision than network with 100 oscillators, suggesting the existence of the collective enhancement of the temporal precision. Near the onset of the synchronization, CV decreases exponentially with respect to R, which is noteworthy and may have an implication for theoretical analysis.

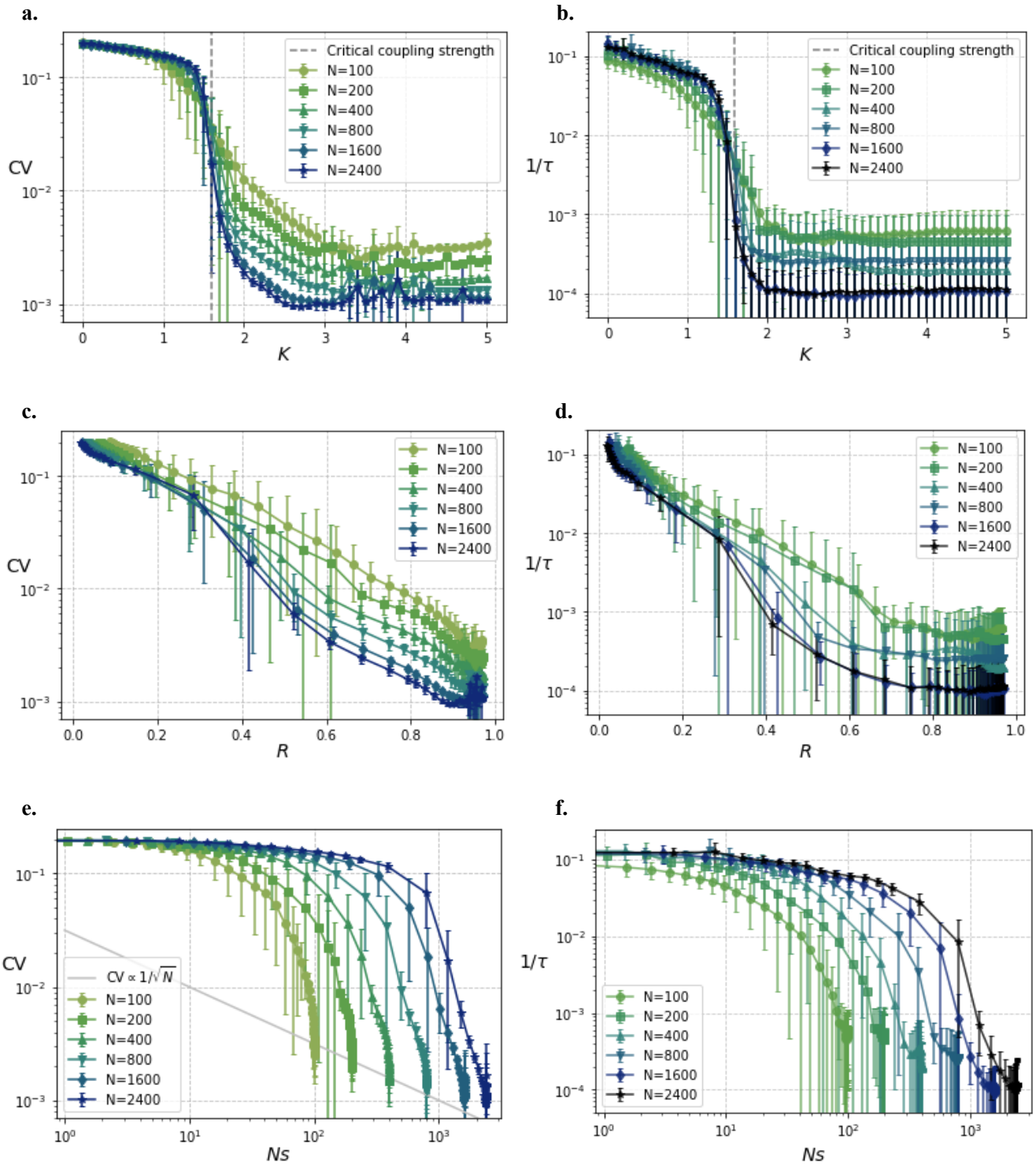

FIG.12 CV and 1/τ of collective oscillation on All-to-all network

Dependence of temporal precision on K and R was investigated for Kuramoto model with the natural frequency $g(\omega) \sim \mathcal{N}(2\pi, 1)$ with different network size N on all-to-all networks. The mean values of 10 trials for different random seeds are shown with the standard deviations.

Dependence of CV (left column) and 1/τ (right column) on the number of synchronized oscillators (Ns) is shown in the lower two figures (Fig.12e and Fig.12f). It is shown that CV and 1/τ decrease as the number of synchronized oscillators increases, i.e., rhythmical precision becomes more precise when more oscillators in the system are synchronized. Temporal precision becomes better when the ratio of synchronized oscillators is near 1. i.e., Ns/N=100/100 gives better temporal precision than Ns/N=100/200, 100/400, 100/800 or 100/1600, and Ns/N =400/400 gives better temporal precision than Ns/N=400/800 or 400/1600.

The proposition of CV$\propto 1/\sqrt{N}$ from the hypothesis of Collective enhancement was verified. As described in the section 2, when the collective oscillation arises, oscillators in Kuramoto model are divided into synchronized group and non-synchronized group, and here the number of synchronized oscillators (Ns) is calculated to know the dependence of CV on Ns or Ns/N ratio.

FIG. 12e. shows CV-Ns curves with diagonal gridline indicating CV$\propto 1/\sqrt{N}$ slopes. The result implies that for each network size N, the endpoint in each curve is found near the CV$\propto 1/\sqrt{N}$ lines. (These endpoints correspond to K=5.0, $KR \simeq 5$, and $Ns \simeq 0.99N$.). That implicates that when most of the oscillators are in the synchronized group and the ratio of Ns/N is near 1, CV obeys the working hypothesis of CV$\propto 1/\sqrt{N}$.

However, as clearly shown in the figure, where the ratio of Ns/N is not near 1, CV-Ns curves do not crawl at all the CV$\propto 1/\sqrt{Ns}$ slope but draw convex curves above the slope. The result implies that CV is not proportional to $1/\sqrt{Ns}$, suggesting that oscillators in the non-synchronized group reduce the rhythmic precision.

4.2 Noisy Kuramoto model

Noisy Kuramoto model was investigated to know the effect of noise on collective oscillation. Fig. 13 shows $1/\tau$-K curves and $1/\tau$-R curves for noisy Kuramoto model with different network size N, on the all-to-all networks.

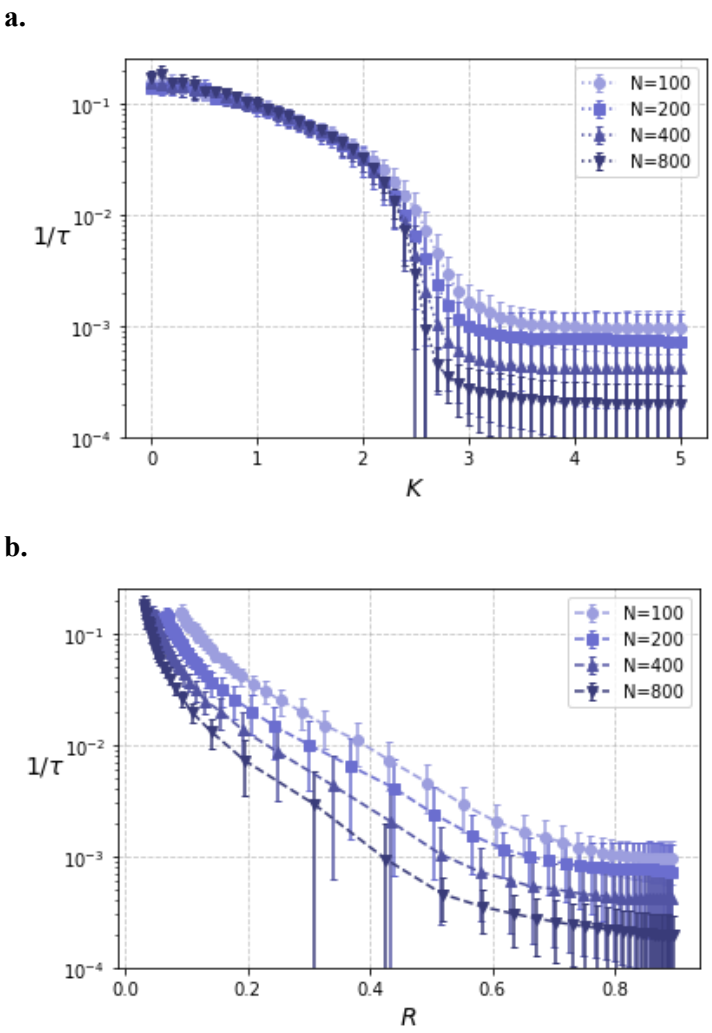

FIG. 13. Temporal precision (1/τ) of collective oscillation in noisy Kuramoto model

Dependence of temporal precision on K and R was investigated for noisy Kuramoto model with natural frequency $g(\omega) \sim \mathcal{N}(2\pi, 1)$ and random gaussian noise $E[\xi_i(t)] = 0$, $E[\xi_i(t)\xi_j(t')] = \delta_{ij}\delta(t-t')$, with the noise strength parameter $\sqrt{D} = 1$. The numerical calculation was conducted by Euler-Maruyama method. The mean values of 10 trials are shown with the standard deviations.

As mentioned above, noise may cause phase-diffusion of self-sustained oscillations and the irregularity of temporal precision, however, mutual interaction of oscillators may recover the phase-diffusion to make synchronization.

Fig. 13a. shows the $1/\tau$-K curves. As shown, $1/\tau$-K curves have reverse-sigmoidal trajectories. When the coupling strength K is larger than the critical coupling strength K_c (K_c<K, in this case $K_c \cong 2.5$ for the phase-disturbance caused by noise), the $1/\tau$ values suddenly becomes small, indicating that synchronization improves the temporal precision, and network with larger system size N had lower $1/\tau$ value, suggesting the existence of the collective enhancement.

Instead, when the coupling strength K is weaker than the critical coupling strength K_c (K>K_c), networks with different network size N had the same trajectories of $1/\tau$-K curves, that is different from that of Kuramoto model (noiseless), however rather like that of noisy-frequency-identical group, as described later.

Fig. 13b. shows the $1/\tau$-R curves. Again $1/\tau$-R curves have similar trajectories as that of frequency-identical group, i.e., $1/\tau$ becomes lower as R becomes larger, indicating that synchronization improves the temporal precision. And network with larger system size N gives lower $1/\tau$ values, suggesting the existence of the collective enhancement of the temporal precision.

4.3 Noisy and frequency-identical oscillators

Fig. 14 shows $1/\tau$-K curves and $1/\tau$-R curves for noisy and frequency-identical phase oscillators with different network size N, on the all-to-all networks.

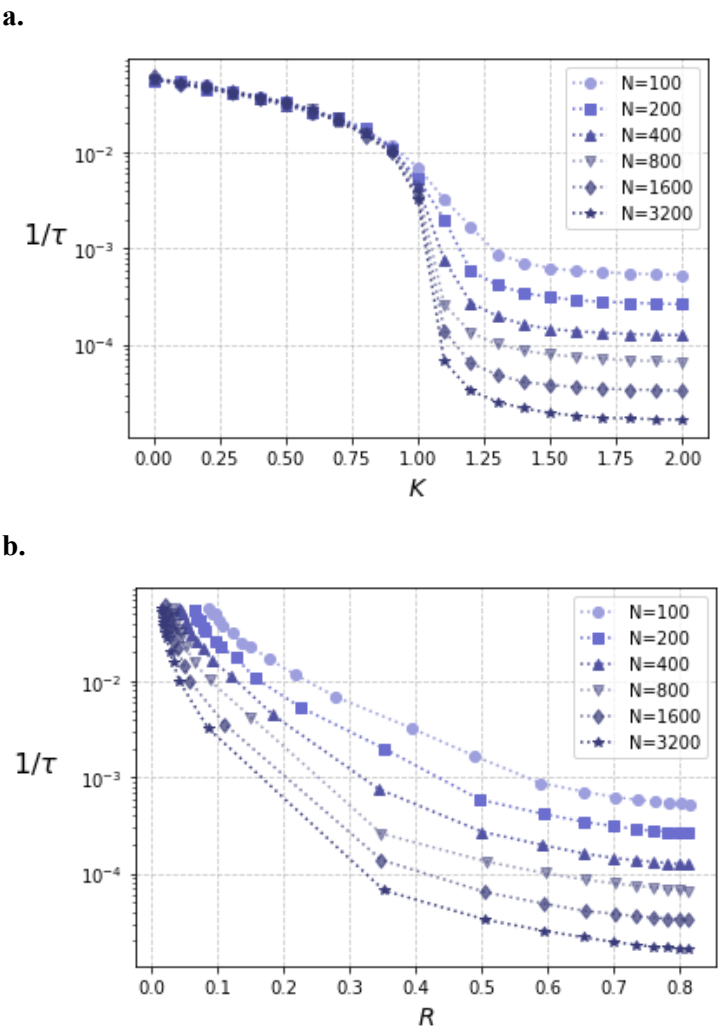

FIG. 14. Temporal precision of noisy phase oscillators with identical frequency

Dependence of temporal precision on K and R was investigated for noisy and frequency-identical phase oscillators. The noise intensity parameter D is set to $\sqrt{D} = 1$. The numerical calculation was conducted by Euler-Maruyama method.

This numerical experiment is set in the similar condition (noisy, frequency-identical) to that in the preceding study Ref. [10]. However, in Ref. [10] very weak noise $\sqrt{D} = 0.01$ was added, to apply the linearization analysis to the phase equation. In this study, the noise was set 10^4 times stronger, $\sqrt{D} = 1$ to investigate the behavior when the noise is sufficiently strong, and the phase equation model cannot be linearized.

FIG. 14a. shows $1/\tau$- K curves. As shown, $1/\tau$-K curves have reverse-sigmoidal trajectories. In the case of noisy-frequency-identical phase oscillators, this is easily comprehensible as there is no dispersion of the natural frequencies of oscillators. $1/\tau$-K curves are same for all network size N when the coupling strength K is sufficiently weak ($K<K_c$, in this case $K_c \cong 1.0$). However, in the condition of $K_c < K$, $1/\tau$-K curves differ depending on the network size N, and the collective enhancement of temporal precision is again observed clearly.

FIG. 14b. shows the $1/\tau$-R curves. $1/\tau$ becomes lower as R becomes larger, suggesting that the temporal precision of the collective oscillation becomes better as the synchronization level becomes higher. And like the former two cases, network with larger system size N gives lower $1/\tau$ values, suggesting the existence of the collective enhancement of the temporal precision.

4.4 Effect of noise

$1/\tau$-R curves in the three mathematical model;

i. Kuramoto model (noiseless).
ii. noisy Kuramoto model; and
iii. noisy and frequency identical phase oscillators.

are compared for various network size N. Fig.15 shows the results.

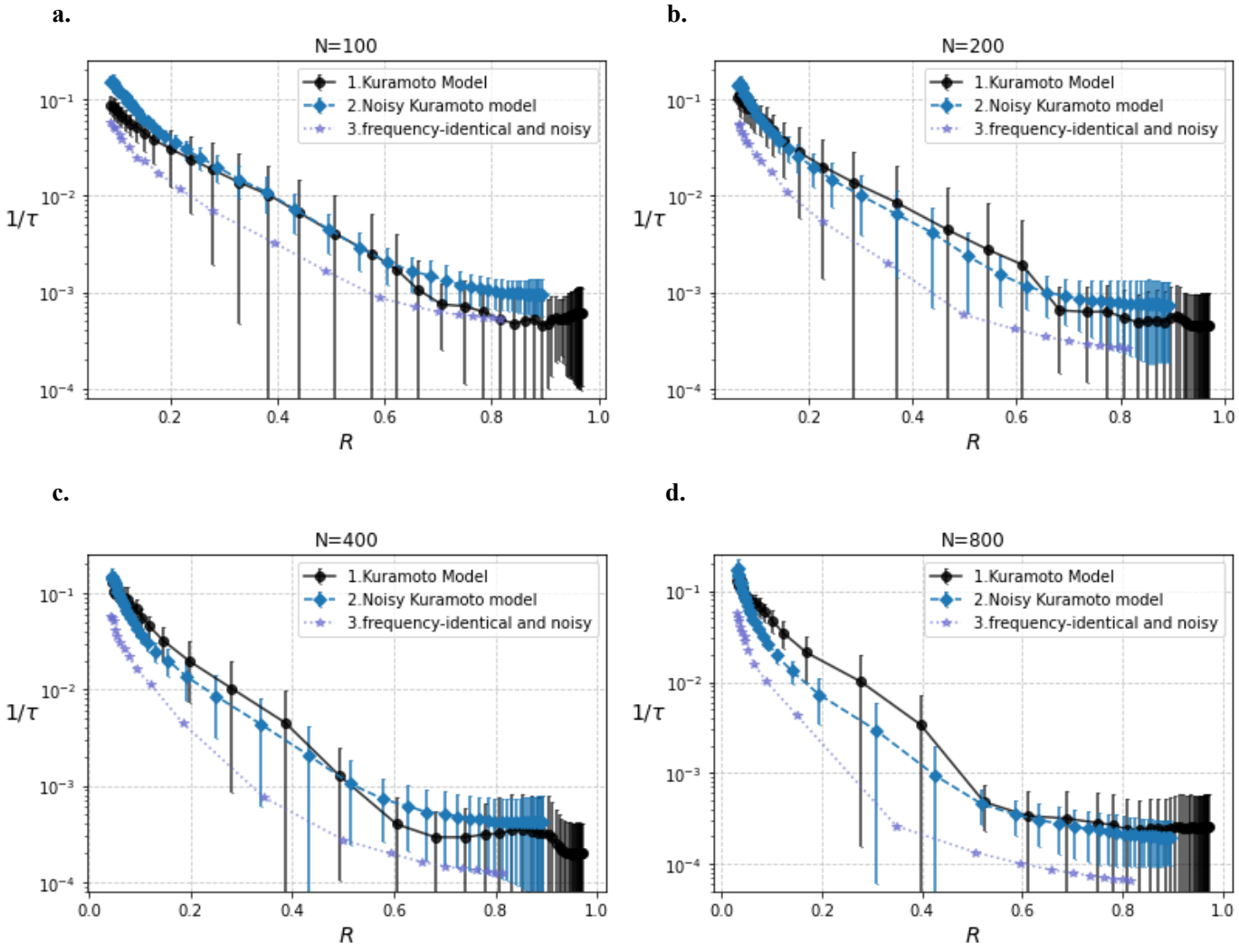

FIG. 15. Effect of Noise on $1/\tau$-R curves

The effect of noise on $1/\tau$-R curves was compared. Kuramoto model (solid lines with circle markers) , noisy Kuramoto model (dashed lines with diamonds markers) and the noisy-frequency-identical phase oscillators (dotted lines with star markers). For I and II the mean values of 10 trials for 10 random seed are shown with the standard deviations. For III, results of 1 trial are shown.

The effect of noise will be known by comparing i. and ii., and the effect of dispersion on natural frequencies will be known by comparing ii. and iii. As shown in the Fig.15, for all network size N, the noisy-frequency-identical oscillators (dotted lines with star markers) had the smallest $1/\tau$ values.

This may be comprehended that the noisy and frequency-identical oscillators, having the same natural frequency (as defined), the independent gaussian white noise added to the third term of the phase equation (12) and (13), i.e., the Wiener process term of the Euler-Maruyama methods, disturb moderately the regulatory of the collective oscillation, while in oscillators in Kuramoto model (noiseless or noisy) the distributed natural frequency (as defined) in the first term of the phase equation (4) more directly affect the regulatory of the collective oscillation and its temporal precision.

When comparing Kuramoto model (noiseless) and noisy Kuramoto model (comparing i. and ii.), the noise effects on $1/\tau$-R curves seem to be different depending on the network size N. Remarkably, when the network size is sufficiently large (N=400,800), the collective oscillation in noisy Kuramoto model had lower $1/\tau$ values than the noiseless Kuramoto model, especially near the oncet of the synchronization (R=0.2~0.4). These results indicate that the independent white gaussian noise term, though added as the Wiener process term to the phase equations, however, have a significant role for the oscillation regulatory, specifically near the onset of the synchronization.

4.5 Dependence on Network Topologies.

Dependence of temporal precision on network topologies was investigated on random network, scale-free network, and small world network. Inquiry of rhythmic precision in Kuramoto model (noiseless) near the onset of the synchronization and regarding the network topology is reported for the first time in this study.

Fig.16. shows the results on random networks.

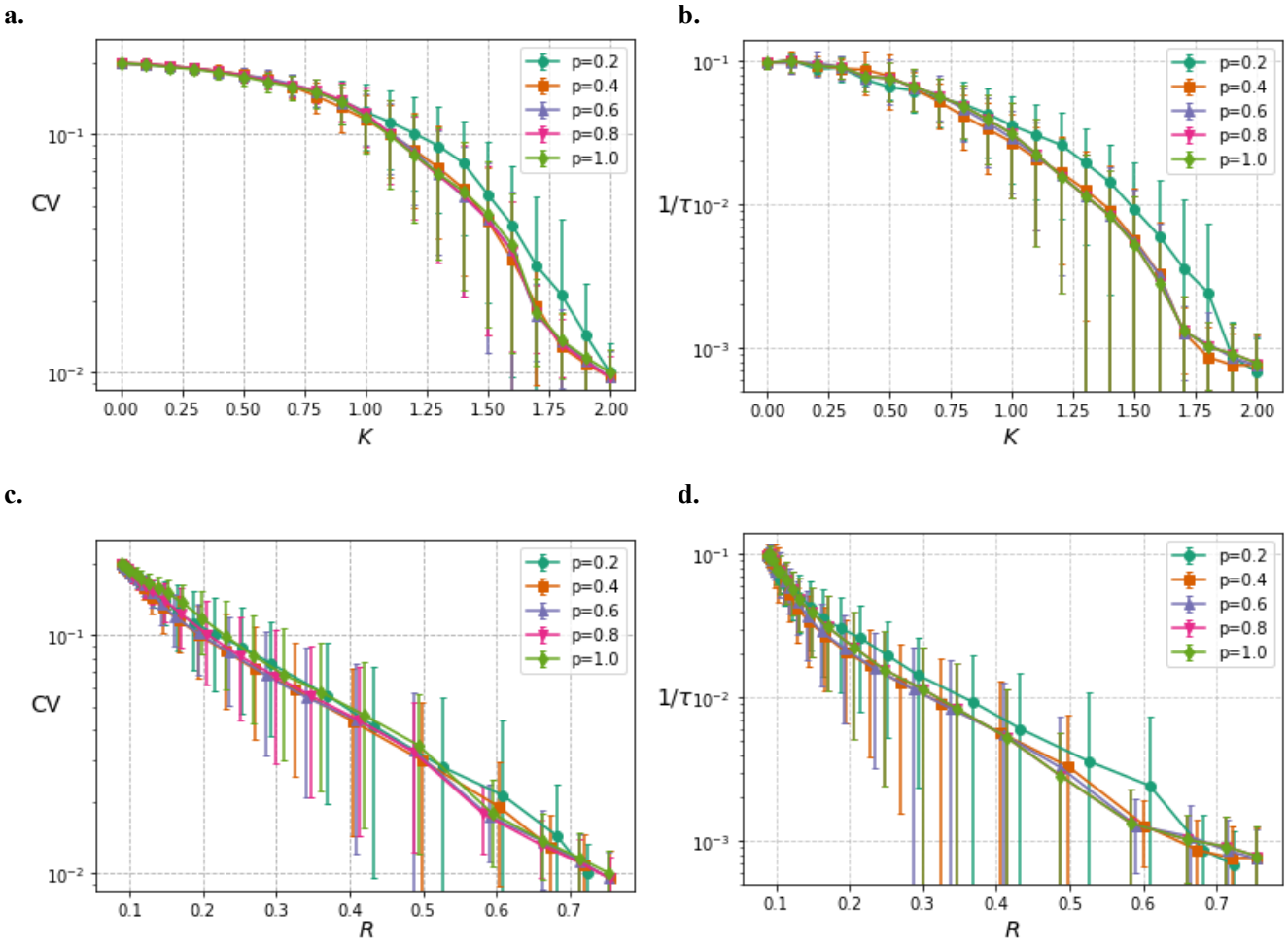

FIG. 16. CV and 1/τ of collective oscillation on Random Network

Dependence of CV (left) and 1/τ (right) on K and R was investigated in Kuramoto model with the natural frequency $g(\omega)\sim\mathcal{N}(2\pi,1)$, on random network with different network topologies. The results are average value of 10 trials for different random seeds. The network size is N=100, and noise term is not added.

Fig.16 shows the dependence of CV (left column) and 1/τ (right column) on the coupling strength K and the synchronization level R on the random network with the average number of links $\langle L\rangle = pN(N-1)/2$. The parameter p indicates a probability of connection. Random network with p=0.2 is the most sparce network, and the random network with p=1.0 is corresponding to all-to-all network.

The result shows that the collective oscillation does not depend on the sparseness on the random network. Both CV-K curves (Fig.16a) and 1/τ-K curves (Fig.16b) as well as CV-R curves (Fig.16c) and 1/τ-R curves (Fig.16d) are similar each other regardless of the difference in p and $\langle L\rangle$, suggesting that dependence of temporal precision on synchronization on random networks resembles that on all-to-all networks, though subtle differences are seen in with the network with p=0.2.

Next, scale-free network was investigated. The scale-free network was built with the parameter m=1 and m=2 and N=100, that means that adding nodes with 1 or 2 link(s) to the existing links and growing the network until the network size N becomes N=100.

FIG.17 shows the dependence of CV (left column) and 1/τ (right column) on the coupling strength K and the synchronization level R on the scale-free networks.

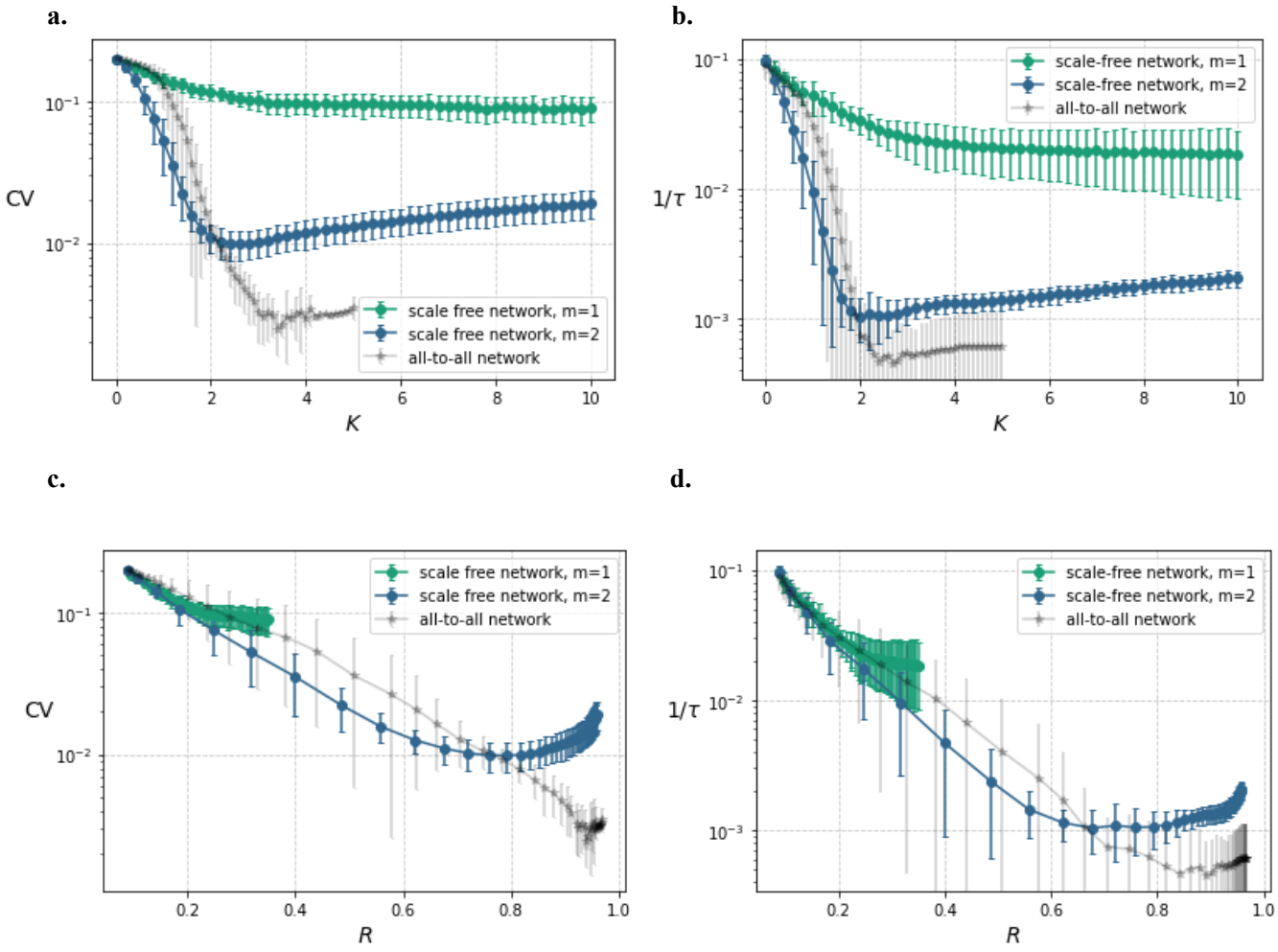

FIG. 17. CV and 1/τ of collective oscillation on Scale Free Network

Dependence of CV (left column) and 1/τ (right column) on K and R in Kuramoto model with the natural frequency $g(\omega)\sim\mathcal{N}(2\pi,1)$, on the scale-free networks with the network parameter m=1 and m=2 was investigated. The default values of networkx (python library) were set for the m0 values. The mean values of 10 trials for different random seeds are shown with the standard deviations. The network size is N=100, noise term is not added.

The result aspects very uniquely. In Fig.17. CV-K curves and $1/\tau$-K curves, as well as CV-R curves and $1/\tau$-R curves for the scale-free network with m=1 (green lines) and m=2 (indigo blue lines) are shown with those of all-to-all network (silver lines) for comparison.

When m=1, CV-K curve and $1/\tau$-K curve for the scale-free network descends as K increase, however approach asymptotically to the certain lower limit. The same tendency is recognizable in CV-R curve and $1/\tau$-R curve. Most notable is that when the coupling strength K is weak (K<1) or the synchronization level R is not high (R=0.2~0.3), that is, the onset of the synchronization, the temporal precision on scale-free network has lower CV and $1/\tau$ values. This means, as a matter of course, that near the onset of the synchronization the collective oscillation on network structure difficult to synchronize has better temporal precision when compared with the same given R value.

When m=2, the observed futures mentioned above for m=1 are more clearly visible. CV-K curve and $1/\tau$-K curve for the scale-free network with m=2 descends as K increase, however approach asymptotically to the certain lower limit, even ascend for stronger K. The same tendency is recognizable in CV-R curve and $1/\tau$-R curve. And clearly, the temporal precision on scale-free network m=2 has lower CV and $1/\tau$ values for wide range of R values (R=0~0.7 or 0.8), not limited to the onset of the synchronization.

The last, small world network was investigated. The small world network was built from the one-dimensional ring lattice connection with average degree $\langle k \rangle = 4$, with the re-wiring parameter p=0.1, 0.2 and 0.5 for network size N =100.

Fig.18 shows the dependence of CV (left column) and 1/τ (right column) on the coupling strength K and the synchronization level R on the small world network.

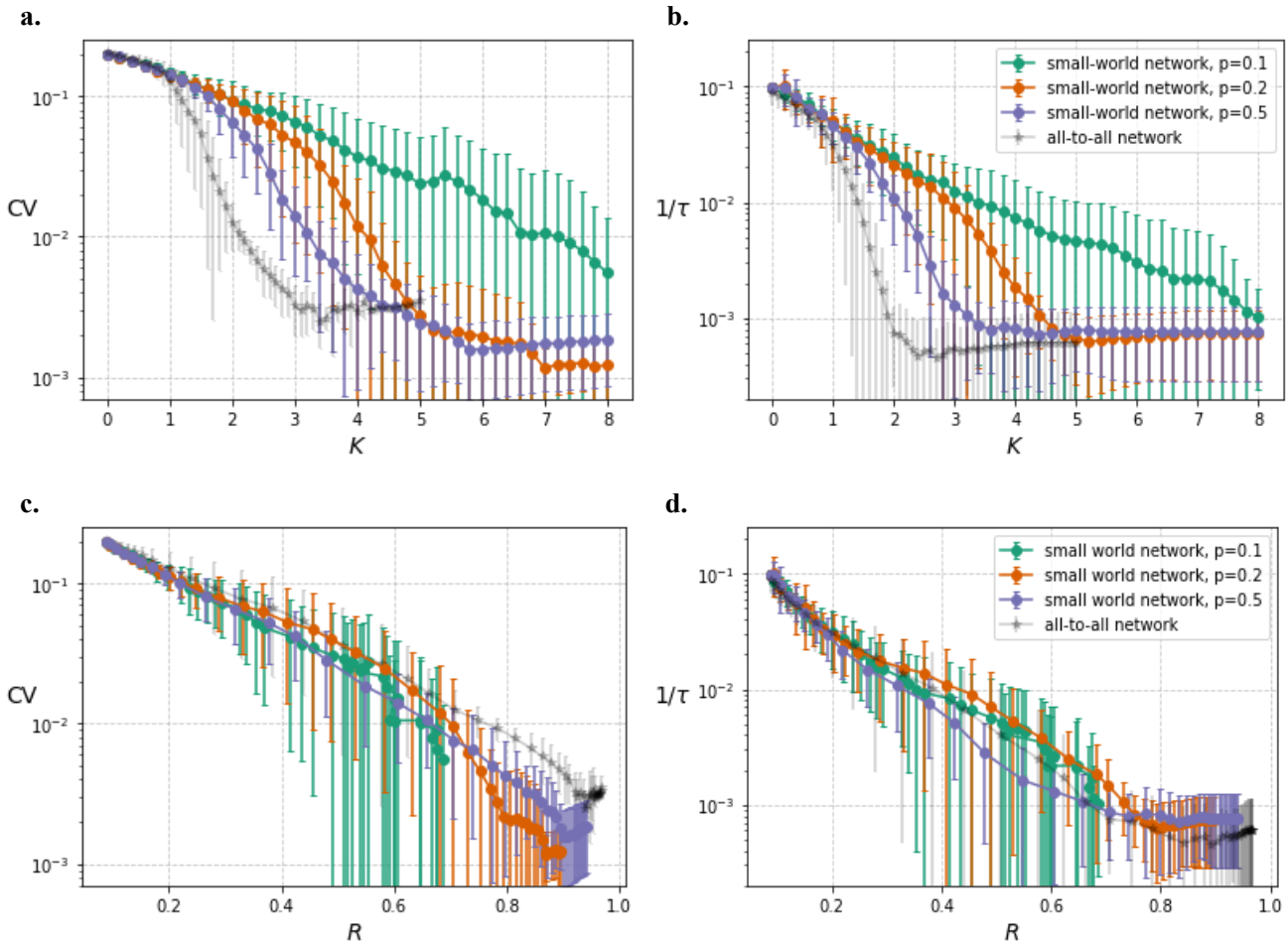

FIG. 18. CV and 1/τ of collective oscillation on Small World Network

Dependence of CV (left column) and 1/τ (right column) on K and R in Kuramoto model with the natural frequency $g(\omega) \sim \mathcal{N}(2\pi, 1)$, on the small world networks with the network parameter p=0.1, 0.2, and 0.5 was investigated. The mean values of 10 trials for different random seeds are shown with the standard deviations. The network size is N=100, noise term is not added.

In Fig.18. CV-K curves and $1/\tau$-K curves, as well as CV-R curves and $1/\tau$-R curves for the small world network with the re-wiring parameter p=0.1 (green lines), p=0.2 (amber lines) and p=0.5 (purple lines) are shown with those of all-to-all network (silver lines) for comparison.

CV-K curves and $1/\tau$-K curves for every small world network descend as K increase, however the trajectories are different depending on the re-wiring parameter p. For stronger K, CV-K curve with p=0.5 cross the CV-K curve with p=0.2, indicating that the rhythmic accuracy of both networks reversed.

CV-R curves and $1/\tau$-R curves for every small world network descend as K increase. Interestingly, CV-R curves resemble each other, even that of all-to-all network. However, for larger R chaotic phenomena are observed.

Section.5 Discussion

In this study dependence of temporal precision on synchronization on oscillator network was investigated in Kuramoto model, noisy Kuramoto model and the noisy phase oscillators with identical frequency, for various network parameters, the network size N, the coupling strength K, and the network topologies.

CV and the reciprocal index $1/\tau$ are used as indicators to examine the temporal precision of rhythmic periodicity of collective oscillation. CV-K curves and/or $1/\tau$-K curves indicate the dependence of temporal precision on the coupling strength K on every oscillator network. CV-K curves and $1/\tau$-K curves descend as K increase, and this tendency is stronger when the network size N is large, suggesting the existence of the collective enhancement of the temporal precision was observed also in this study. The progressing of temporal precision grows near K_c., that indicates that synchronization improves the temporal precision.

As shown in the Fig.12 there is a reciprocal intersection of CV-K curves or $1/\tau$-K curves near K_c, such that when $K<K_c$, smaller network has more precise periodicity, where $K_c<K$, larger network has more precise periodicity. The intersection is seen only in Kuramoto model (noiseless).

One possible explanation is that this phenomenon is caused by another reciprocal intersection in R-K curves. Remark that in Fig.3 in Kuramoto model, near K=1.8, N-dependent R-K curves have the same intersection. When K is far smaller than K_c the network with minimum network size (N=100) gives the highest R value, however, under the condition of $K>K_c$, oppositely, the largest network (N=2400) has the highest R value. This kind of reciprocal intersection is not seen in R-K curves of noisy Kuramoto model and noisy-frequency-identical phase oscillators, that is well consistent with such suggestion, that in these two models, the intersection is not seen at all in CV-K curves nor $1/\tau$-K curves.

CV-R curves and $1/\tau$-R curves indicate the dependence of temporal precision on the synchronization level on every oscillator network. CV-R curves and $1/\tau$-R curves descend as R increase in all three cases, Kuramoto model, noisy Kuramoto model and the noisy-frequency-identical phase oscillators, however the curve slopes or differential coefficients differ according to the model or the network topologies. In Kuramoto model (noiseless) on the all-to-all network the progressing of temporal precision is not constant but accelerated near R=0.3~0.4 (Fig.12c)

when the network size N is large (N=800 and 1600).

The working hypothesis of CV$\propto 1/\sqrt{N}$ or CV$\propto 1/\sqrt{Ns}$ was verified in the Kuramoto model (noiseless) on the all-to-all network to know the dependence of CV on Ns or Ns/N ratio. As shown in FIG. 12e, CV-Ns curves do not crawl at all the CV$\propto 1/\sqrt{Ns}$ slope but draw convex curves above the slope. The result indicates that oscillators in the non-synchronized group reduce the rhythmic precision.

Dependence of temporal precision on the network topologies was investigated in random networks, scale-free networks, and small world networks. The results contained a lot of information. Oscillatory networks on the random network, having R-K curves that is similar to those on all-to-all network, had almost same temporal precision as that of all-to-all network, regardless of the sparseness.

Scale-free networks had variety of rhythmic precision, when m=1 the temporal precision was not good, however when the network parameter was changed to m=2, the temporal precision significantly improved, and showed even better temporal precision than those on the all-to-all network. Small world network had yet another nature of temporal precision, depending on the re-wiring parameter p. The difference between the scale-free network and the small-world network may be comprehended in such a manner that in the scale-free network graph node order is power distributed, whereas not power distributed in the small world network.

In the last, let me introduce yet another point of issue related to the oscillation regulatory.

Biological rhythms are stable. This stability is called homeostasis. And stable rhythms are widely found. Synchronization is a bifurcation phenomenon, while self-consistency theory cannot determine if the collective oscillation obtained as a solution of Kuramoto model is stable or not.

A phase dispersion function $f(\phi,t,\omega)$ for ensemble of oscillators has seemingly infinite degrees of freedom as a function of phase ϕ, however it can be reduced to a dynamical system with only three degrees of freedom by the Watanabe & Strogatsz transformation (W-S transformation) [39]. And Ott & Antonsen argue that restricting the dynamics of the phases to individual ω to Poisson submanifolds (2-dimensional) on 3-dimensional invariant manifolds obtained by the W-S transformation still gives a correct view on the collective properties of the

system. Based on these hypotheses, an evolution equation for the complex order parameter Z in the thermodynamic limit of $N \to \infty$ in the form of the SL equation can be obtained and it is concluded that the synchronization transition is stable in a certain range [40].

In this study the author assumed that the synchronization is stable along with the Ott & Antonsen theory. The stability of synchronization long had been an unresolved proposition, finally solved by Chiba et al [41,42].

In the meantime, interesting result is reported related on the fluctuations of rhythm and the effects of noise [43]. The author will continue the study to inquire the unknown nature of synchronization and rhythmic precision of oscillation regulatory.

Section.6 Acknowledgements

The author is grateful with Professor Hiroshi Kori for the teaching, discussion, and supervision of the Master Program Study, and the Master's Thesis.

The author thanks gratefully the members of the Nonlinear Physics Group (Kori-Kobayashi-Izumida group) for the discussion and consultation.

Section.7 References

1. A. T. Winfree, *J of Theor. Biol* **16** (1967) 15
2. A. T. Winfree, *The Geometry of Biological Time* (Springer-verlag, New York, 1980, 2nd Edition, 2001)
3. Y. Kuramoto, *Chemical Oscillations, Waves, and Turbulence*. (Springer, New York. 1984)
4. A. *Pikovsky, M. Rosenblum, and J. Kurths, Synchronization -A Universal Concept in Nonlinear Science-* (Cambridge University Press, New York, 2001) 『同期理論の基礎と応用』丸善 2009
5. S.H. Strogatz, *Sync: How Order Emerges from Chaos in the Universe, Nature and Daily Life* (Hyperion Books, New York, 2003)『SYNC』早川書房 2005
6. H. Sakaguchi and Y. Kuramoto, Prog. Theor. Phys. **76** (1986) 576.
7. 蔵本由紀, 河村洋史 (著)『同期現象の科学』京都大学学術出版会 2017
8. 蔵本由紀 (著) 『非線形科学』集英社新書 0408G 2007
9. 蔵本由紀 (著) 『非線形科学 同期する世界』集英社新書 0737G 2014
10. H. Kori, Y. Kawamura, N. Masuda, Journal of Theoretical Biology **297** (2012) 61–72
11. K. Moortgat, T. Bullock, T. Sejnowski, (2000a). J. Neurophysiol. **83** (2), 984–997., (2000b). J. Neurophysiol. **83** (2) 971–983.
12. J. R. Clay, R. L. DeHaan, 1979, Biophysics J., **28** (3) 377-389
13. W. Rappel, A. Karma 1996, Phys. Rev. Lett. **77** (15), 3256-3259
14. D. J. Needleman, P. H. E. Tiesinga, T. J. Sejnowski, 2001.Physica D **155**, 324–336
15. 森肇, 蔵本由紀 (著)『散逸構造とカオス』岩波書店 1994
16. 蔵本由紀, 河村洋史 (著)『同期現象の数理；位相記述によるアプローチ』培風館 2010
17. 蔵本由紀 (編)『リズム現象の世界』東京大学出版会 2005
18. 郡宏, 森田善久 (著) 『生物リズムと力学系』共立出版 2011
19. H. Daido, J. Stat. Phys. **60** (1990) 753
20. A Pikovsky, S. Ruffo, 1999 Phys. Rev. E, **59** (2)
21. Y. Kawamura, Phys. Rev. E. **76**. (2007) 047201
22. M. Komarov and A. Pikovsky. Phys. Rev. E Stat. Nonlin. Soft Matter Phys. **92**.2 (2015)
23. F. Peter, C. C. Gong, and A. Pikovsky.: Phys. Rev. E **100** (2019) 032210
24. F. Peter, A. Pikovsky, .: Phys. Rev. E **97** (2018) 032310
25. Gerstner, W., Kistler, W., (2002). Spiking Neuron Models: Single Neurons, Populations, Plasticity. Cambridge University Press, Cambridge
26. A. Arenas, A. Diaz-Guimera, J. Kurths, Y. Moreno, C. Zhou, Physics Reports **469** (2008) 93-153
27. 増田直紀, 今野紀雄(著) 『複雑ネットワーク - 基礎から応用まで - 』近代科学社 2010

28. A. Barabasi (著) 京都大学ネットワーク社会研究会(訳)『ネットワーク科学』共立出版 2019
29. Rodrigues et al., Physics Reports **610** (2016) 1–98
30. Restrepo, Ott, and Hunt, Phys. Rev E **71** (2005) 036151
31. Juan G. Restrepo, Edward Ott, Brian R. Hunt, CHAOS **16** (2006) 015107
32. H. Sakaguchi, S. Shinomoto, Y. Kuramoto.: Progress of Theoretical Physics **77** (1987) 1005-1010, Progress of Theoretical Physics **79** (1988) 1069-1079
33. H. Kori, A. S. Mikhailov, Phys. Rev. Lett. **93** (2004) 254101; Phys. Rev E **74** (2006) 066115
34. T. Ichinomiya, 2004, Phys. Rev. E **70**, 026116
35. P. Erdos and A. R¨enyi, Publ. Math. Debrecen **6**, (1959) 290-297
36. A. Barabasi L, R. Albert, Nature **401** (1999) 130-131
37. A. Barabasi L, R. Albert, Science, **286** (1999) 509-512
38. D. J. Watts and S. H. Strogatz, Nature **393** (1998) 440
39. S. Watanabe, S. H. Strogatsz, Phys. Rev. Lett. **70**, (1993) 2391, Physica D **74** (1994) 197
40. E. Ott and T.M. Antonsen, Chaos **18**, (2008) 037113
41. H. Chiba: Ergodic Theory and Dynamical Systems (2013)
42. H. Chiba: 2011, 2016, 2018, 2020
43. J.H. Meng, H. Riecke, Scientific Reports **8** (2018) 6949